reactions

MDPI

Supplementary Materials

Condensed Phase Guerbet Reactions of Ethanol/Isoamyl Alcohol Mixtures

Iman Nezam [1,2,*], Lars Peereboom [2], and Dennis J. Miller [2]

[1] School of Chemical and Biomolecular Engineering, Georgia Institute of Technology, Atlanta, GA. 30318
[2] Chemical Engineering and Materials Science Department, Michigan State University, East Lansing, MI. 48824; peereboo@egr.msu.edu (L.P.); millerd@egr.msu.edu (D.J.M.)
* Correspondence: inezam3@gatech.edu

Received: date; Accepted: date; Published: date

Contents

1. Development of Kinetic Model from "Indirect" Guerbet Reaction Mechanism

1.1. Ethanol condensation to butanol (from ref 24)

The indirect mechanism for ethanol condensation to higher alcohols involves several steps, the first two of which are

Ethanol (*E*) dehydrogenation to acetaldehyde (*AA*): $E = AA + H_2$ (RS1)
Acetaldehyde (*Ac*) condensation to crotonaldehyde (*CA*): $2\,AA \rightarrow CA + H_2$ (RS2)

As seen above, ethanol dehydrogenation is a catalytic, reversible reaction that occurs on the metal surface sites, while acetaldehyde condensation is an irreversible reaction that takes place on the basic sites of the catalyst.

$$r_{S1} = -r_E = k_{S1}(C_E - \frac{C_{AA}C_{H2}}{K_{eS1}C_{soln}}) \quad \text{(ES1)}$$

$$r_{S2} = k_{S2}C_{AA}^2 \quad \text{(ES2)}$$

If ethanol condensation to *n*-butanol is the only reaction taking place, then $C_{AA} \approx C_{H2}$, since each mole of hydrogen liberated by ethanol dehydrogenation is consumed in hydrogenation of *CA*. Although not exact, this equality is a useful approximation for development of the kinetic model that focuses on condensation reactions.

At steady state, the rates of (RS1) and (RS2) are related to each other by $r_{S1} = 2r_{S2}$. Applying this equality of rates and solving for C_{AA}^2 gives the following:

$$C_{AA}^2 = \frac{k_{S1}\, C_E}{(2k_{S2} + k_{S1}/K_{eS1}C_{soln})} \quad \text{(ES3)}$$

Inserting this expression into r_2 and rearranging gives a final expression for the rate of ethanol consumption.

$$-r_E = 2r_{S2} = \frac{C_E}{\left(\frac{1}{k_{S1}} + \frac{1}{2k_{S2}K_{e1}C_{soln}}\right)} \quad \text{(ES4)}$$

This expression includes rate constants for the first two steps of the indirect Guerbet mechanism for reaction of *E* to the C4 product, and the equilibrium constant K_{eS1} for (RS1). It simplifies if one of the two reaction steps is rate limiting, but remains first order in ethanol regardless of which step is rate limiting.

1.2. Mixed EtOH/IAOH condensation reactions

In addition to (RS1) and (RS2), the following reactions take place in the indirect Guerbet reaction mechanism when isoamyl alcohol (IA) is present along with E at beginning of reaction.

Isoamyl alcohol (*IA*) dehydrogenation to 3-methyl-butanal (*MB*): $IA = MB + H_2$ (RS3)

Cross condensation of *AA* with *MB* to form C7 aldehyde product: $AA + MB = C7A$ (RS4)

Self-condensation of *MB* to form C10 aldehyde product: $MB + MB = C10A$ (RS5)

The rate expressions for each of these mechanistic steps are as follows:

$$r_{S3} = k_{S3}\left(C_{IA} - \frac{C_{MB}C_{H2}}{K_{eS3}C_{soln}}\right) \quad \text{(ES5)}$$

$$r_{S4} = k_{S4}C_{AA}C_{MB} \quad \text{(ES6)}$$

$$r_{S5} = k_{S5}C_{MB}^2 \quad \text{(ES7)}$$

The conversion of IA occurs predominantly via cross condensation with E, so at steady state $r_{S3} \approx r_{S4}$. Hydrogen is generated by both RS1 and RS3, but because the concentration of E is greater than that of IA, and the conversion rate of E is greater than that of IA, hydrogen generation is dominated by RS1. Thus $C_{H2} \approx C_{AA}$, and equating r_{S3} and r_{S4} gives:

$$C_{AA}C_{MB} = \frac{k_{S3}C_{IA}}{k_{S4} + k_{S3}/K_{eS3}C_{soln}} \quad \text{(ES8)}$$

Substituting this expression into (ES6) gives:

$$r_{C7} = r_{S4} = \frac{C_{IA}}{\left(\frac{1}{k_{S3}} + \frac{1}{k_{S4}K_{eS3}C_{soln}}\right)}$$

Thus under the experimental conditions of this study, with initial concentration of E greater than that of IA, the cross condensation reaction is solely first order in IA. A similar analysis of C10

product formation (RS3 and RS5) shows that reaction also to be first order in IA. Finally, the secondary reaction of BuOH (C4) with E, given as R4 in the body of the manuscript, also becomes first order in C4 at conditions of this study. The final forms of the rate expression are shown in Table S1 below.

Table S1. Rate expressions for Reactions (R1) – (R6) in kinetic model

Reaction	Rate Expression
R1	$r_1 = \frac{k_1 C_E}{1 + K_W C_W}$
R2	$r_2 = \frac{k_2 C_{IA}}{1 + K_W C_W}$
R3	$r_3 = \frac{k_3 C_{IA}}{1 + K_W C_W}$
R4	$r_4 = \frac{k_4 C_{C4}}{1 + K_W C_W}$
R5	$r_5 = \frac{k_5 C_E}{1 + K_W C_W}$
R6	$r_6 = \frac{k_6 C_{IA}}{1 + K_W C_W}$

1.3. Calculation of Water Concentration

Final water concentration was determined in every experiment via triplicate Karl-Fischer analysis. In the model simulation, product water formation was calculated from the stoichiometry of Guerbet reactions, and from the side reactions of both E and IA. Because there are multiple reactions collectively considered as forming "other" products in the model, a stoichiometric factor of water formation was assigned to match as closely as possible the experimental product water concentration. The value used for the factor was 0.3 mol H_2O formed per mole E or IA consumed in reaction to "other" products.

2. Evaluation of Intraparticle Mass Transport Resistances

The influence of intraparticle mass transport on ethanol conversion at 250 °C (and lower temperatures) for the nickel catalyst can be evaluated via calculation of the observable modulus $\eta\varphi^2$ at the continuous reactor inlet at 250 °C.

$$\eta\varphi^2 = \frac{-r_E L^2}{D_e C_{Eo}}$$

Where $-r_E$ = ethanol consumption rate at reactor inlet = 6 x 10^{-3} kmol E/m^3 cat/sec
L = normalized catalyst particle size = D/6; D = 1.6 x 10^{-3} m
D_e = effective condensed-phase diffusivity of EtOH in IAOH = 2.3 x 10^{-9} m^2/sec
C_{Eo} = Inlet concentration of ethanol at 250 °C and 100 bar, = 6.9 kmol E/m^3

The inlet ethanol reaction rate is determined by calculating the average ethanol rate at 250 °C and WHSV = 2.1 h^{-1} and scaling it from average ethanol concentration in the reactor to the inlet ethanol concentration. The effective diffusivity is calculated from the Wilke-Chang equation, and multiplied by the catalyst particle porosity squared according to the random pore model. Inlet concentration of EtOH is taken from Table S2.

The calculated value of the observable modulus ηφ2 at the reactor inlet for the nickel catalyst at 250 °C is less than 1.0, indicating that intraparticle mass transfer limitations have a most a modest effect on reaction rates at the experimental conditions of this work.

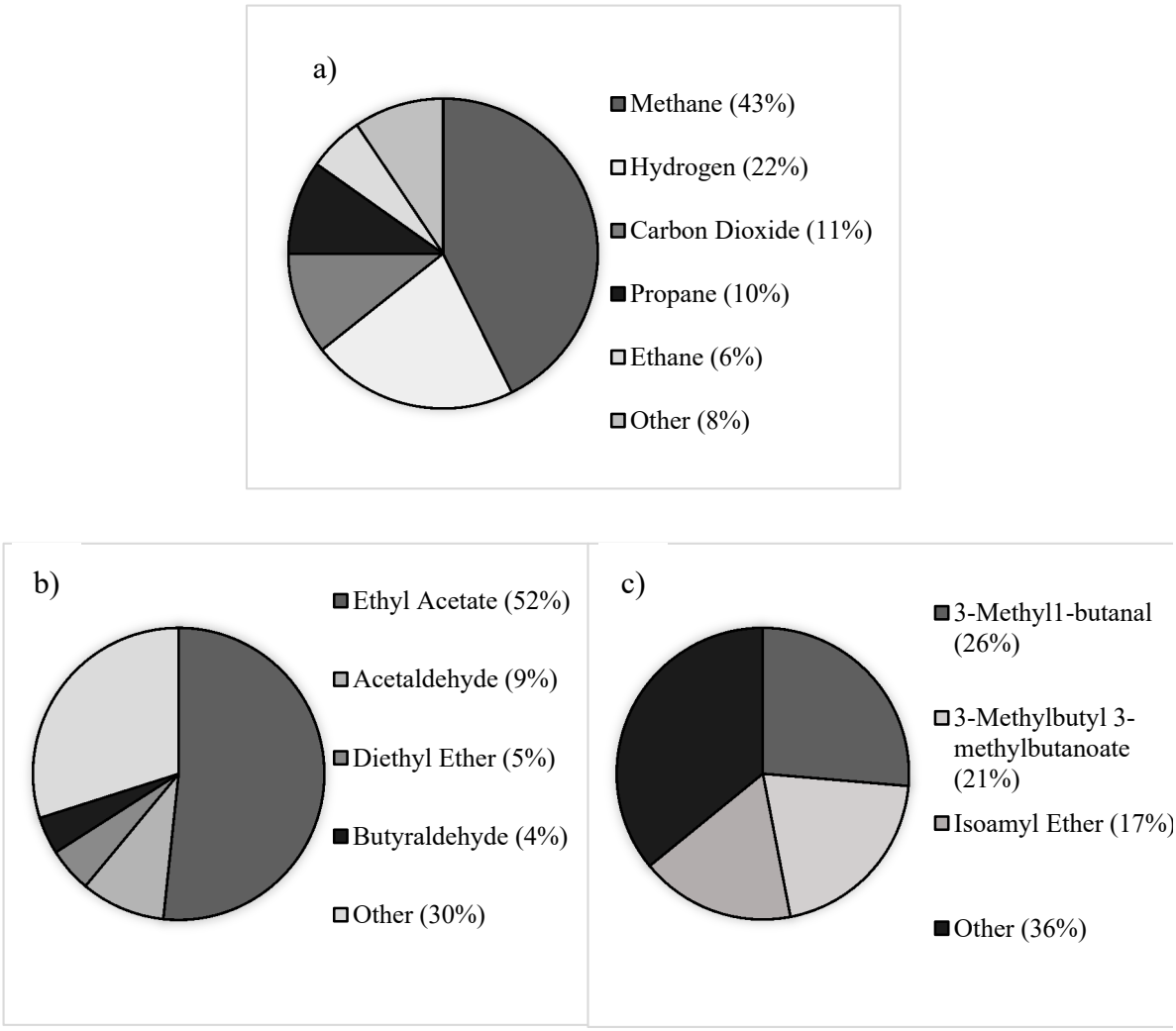

Figure S1. Typical molar compositions of liquid and gas byproducts formed in Guerbet reactions of EtOH and IAOH: a) gas; b) EtOH; c) IAOH.

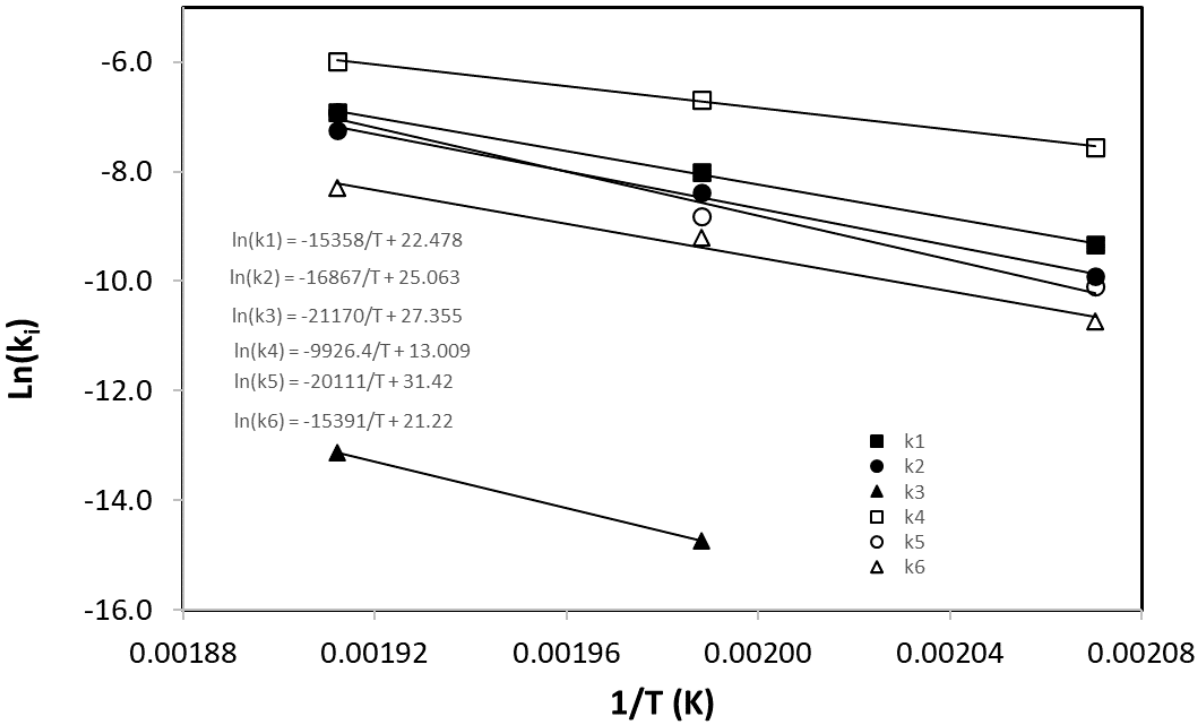

Figure S2. Arrhenius plots for rate constants in kinetic model.

Table S2. Inlet concentrations of EtOH (E) and IAOH (IA) in continuous reactor. Initial molar feed ratio is E:IA = 3.83:1 for all continuous flow reactor experiments.

Temperature	$C_{E,o}$	$C_{IA,o}$
(°C)	(kmol/m³)	(kmol/m³)
210	10.27	2.68
230	8.68	2.27
250	6.91	1.80

Table S3. Comparison of experimental and simulated outlet concentrations from continuous flow reactor.

T	τ		C_E	C_{IA}	C_{C10}	C_{C4}	C_{C6+C8}	C_{C7+C9}	C_{Eother}	$C_{IAother}$
(°C)	(h)		(kmol/m³)							
210	0.37	Exp	9.672	2.660	0.00000	0.186	0.013	0.033	0.158	0.000
		Model	9.712	2.635	0.00004	0.195	0.012	0.031	0.097	0.014
	0.54	Exp	9.467	2.624	0.00000	0.267	0.026	0.042	0.148	0.015
		Model	9.538	2.621	0.00006	0.250	0.021	0.041	0.126	0.018
	0.96	Exp	9.230	2.586	0.00000	0.347	0.046	0.064	0.141	0.030
		Model	9.173	2.591	0.00009	0.355	0.052	0.062	0.187	0.027
230	0.31	Exp	7.575	2.111	0.00000	0.372	0.052	0.071	0.126	0.083
		Model	7.550	2.153	0.00014	0.374	0.038	0.078	0.187	0.034
	0.45	Exp	7.194	2.145	0.00012	0.444	0.070	0.101	0.282	0.019
		Model	7.250	2.122	0.00017	0.456	0.060	0.099	0.235	0.043
	0.82	Exp	6.647	2.052	0.00030	0.590	0.115	0.147	0.349	0.065
		Model	6.652	2.061	0.00025	0.600	0.119	0.142	0.327	0.062
250	0.25	Exp	4.755	1.606	0.00029	0.511	0.112	0.133	0.658	0.065

	Model	4.977	1.639	0.00034	0.512	0.069	0.122	0.581	0.042
0.36	Exp	4.278	1.557	0.00048	0.602	0.154	0.173	0.782	0.073
	Model	4.548	1.599	0.00042	0.598	0.104	0.151	0.702	0.053
0.65	Exp	3.981	1.589	0.00058	0.702	0.161	0.189	0.841	0.025
	Model	3.730	1.517	0.00059	0.730	0.194	0.212	0.925	0.074

Table S4. Initial concentrations of EtOH (E) and IAOH (IA) in batch reactions (230 °C).

Experiment	$C_{E,o}$ (kmol/m^3)	$C_{IA,o}$ (kmol/m^3)
B2	13.31	0
B3	8.63	2.27
B5	4.35	4.35
B4	1.44	5.77
B6	0	6.47
B7	8.63	2.27

Table S5. Comparison of experimental and simulated species final concentrations for batch reactions at 230 °C.

Exp	Reaction Time (h)		C_{EtOH}	C_{IAOH}	C_{C10}	C_{C4}	C_{C6+C8}	C_{C7+C9}	C_{Eother}	$C_{IAother}$
			(kmol/m^3)							
B2	22	Exp	10.50	0	0	0.948	0.253	0	0.154	0
		Model	11.12	0	0	0.743	0.105	0	0.386	0
B3	23	Exp	6.03	1.96	0	0.660	0.163	0.177	0.634	0.134
		Model	6.84	2.09	0	0.546	0.094	0.126	0.291	0.055
B5	22	Exp	2.82	3.86	0.0021	0.299	0.064	0.286	0.479	0.206
		Model	3.28	4.00	0.0004	0.270	0.047	0.243	0.144	0.105
B4	24	Exp	0.82	5.21	0.0089	0.080	0.025	0.261	0.127	0.280
		Model	0.792	5.23	0.0006	0.088	0.019	0.370	0.049	0.161
B6	24	Exp	0	5.75	0.0173	0	0	0	0	0.683
		Model	0	6.16	0.0122	0	0	0	0	0.306
B7	51	Exp	5.14	1.94	0.0009	0.837	0.227	0.237	0.930	0.092
		Model	5.98	2.00	0.0003	0.722	0.201	0.189	0.419	0.082